胞の L-Glu トランスポーターの発現制御に関して報告はほとんどない。今後、ミクログリアから産生される液性因子の解明を行う。また、ミクログリア添加自体によって、脳内 L-Glu 濃度上昇が引き起こされている可能性についても確認する必要がある。

2. ヒト iPS 細胞由来神経細胞による in vitro 神経毒性評価系の完成

2-1. ヒト iPS 細胞由来神経細胞に最適化した毒性評価プロトコルの確立

従来の齧歯類初代培養神経細胞に用いられてきた細胞毒性評価プロトコルをヒト iPS 細胞由来神経細胞用に最適化した。ヒト iPS 細胞由来神経細胞は齧歯類初代培養細胞に比較し、非常にはがれやすい。また、結果は示していないが、従来のプロトコルでは PI 暴露時間が 24 時間となっており、同じ条件でヒト iPS 細胞由来神経細胞を染色したところ、PI 暴露のみでほとんどの細胞が死滅してしまった。PI は DNA の二重らせん構造に intercalate することにより特有の赤色蛍光（620 nm）が増強される。生細胞と死細胞が共存している条件では、細胞膜が侵襲をうけている死細胞のみにとりこまれ、蛍光を発するとされている。これまで、PI 自体に毒性が報告された例はなく、そのメカニズムは不明であるが、ヒト iPS 細胞の細胞毒性を評価する際には、齧歯類初代培養神経細胞で用いられている検出系の条件をマイルドにする必要があると考えた。条件検討を繰り返し、Fig. 3A で示すヒト iPS 細胞由来神経細胞に最適化した細胞毒性プロトコルを確定した。

2-2. ヒト iPS 細胞由来神経細胞の興奮毒性の検出能力の検証

中枢神経系において、神経細胞どうしはシナプスという構造で接合している。シナプスは、特定条件で興奮性神経伝達物質グルタミン酸の放出確率が上昇するといった、伝達効率の変化＝シナプス可塑性を生み出すマシナリーがあり、記憶や学習といった高次中枢神経機能の基盤となっている。その一方で、シナプス可塑性に関わる NMDA 型グルタミン酸受容体が、過剰なグルタミン酸刺激によって引き起こされる興奮毒性の原因となっている。興奮毒性は神経特異的な毒性メカニズムであり、実は非常に多くの神経障害共通のメカニズムとなっている。今回我々は、L-Glu に対するカルシウム応答に NMDA 受容体成分が含まれない 253G1 由来神経細胞標本では興奮毒性が再現できず、NMDA 成分が含まれる iNeuron では興奮毒性を再現できた。これらの結果は、医薬品等が興奮毒性を引き起こすかどうかの評価ではカルシウムイメージング等で 機能的 NMDA 受容体発現が保証された標本を選別して使用する必要があることを示唆する重要なデータである。

2-3. シナプス機能障害の定量評価化法

これまで医薬品の中枢神経機能への有害影響については、ほとんど丸ごと動物を用いた in vivo 評価が用いられてきた。しかし、中枢神経研究の進歩により高次機能の変化と相関のある細胞レベルでの変化が数々見いだされている。その一つがシナプス機能を反映した、シナプス後部のスパイン形態の変化とスパインにクラスターするアクチン結合タンパク質ドレブリンの分布である（Takahashi et al., J Neurosci 23, 6586-6595, 2009）。我々は今回、ドレブリンのスパイン一樹状突起分布を SDR という指標を設定することにより定量化することに成功した（Mizui et al., PLOS ONE 9(1) e85367, 2014）。また、この SDR がシナプス機能に影響を与える条件の L-Glu 刺激によって低下することも確認した。これらの結果は高次機能への有害影響

を、SDR を用いて予測できる可能性を示している。今後はすでに中枢影響が明らかな種々の実験条件や医薬品等を用いて、SDR の高次機能への影響予測性についてデータを集積する必要がある。また、ヒト iPS 細胞由来神経細胞における SDR 算出にも取り組む。

E. 結論

・従来の in vitro BBB モデルにミクログリアを添加することにより、より強固なバリア機能を実現した。その根拠となるメカニズムの一部を明らかとした。

・PI/calcein イメージング、LDH/MTT 同時測定法の細胞毒性評価プロトコルをヒト iPS 細胞由来神経細胞に最適化した。

・NMDA 受容体を発現していなければ興奮毒性評価は困難であり、そのためのヒト iPS 細胞由来神経細胞標本の選別が重要である。

・シナプス機能障害定量評価法として、アクチン結合タンパク質ドレブリンの局在変化を指標とできることを見いだした。

F. 研究発表

1. 論文発表

1. Mizui T., Sekino Y., Yamazaki Y., Ishizuka H., Takahashi H., Kojima N., Kojima M., Shirao T. Myosin II ATPase activity mediates the long-term potentiation-induced exodus of stable F-actin bound by drebrin A from dendritic spines" PLOS ONE 9(1) e85367 (2014)

   http://www.plosone.org/article/info%3Adoi%2F10.1371%2Fjournal.pone.0085367

2. Shigemoto-Mogami Y., Hoshikawa K., Goldman J.E., Sekino Y., Sato K. (2014) Microglia enhance neurogenesis and oligodendrogenesis in the early postnatal subventricular zone. J Neurosci 34(5), 2231-2243

3. Yamazaki H., Kojima N., Kato K., Hirose H., Iwasaki T., Mizui T., Takahashi H., Hanamura K., Roppongi R.T., Koibuchi N., Sekino Y., Mori N., Shirao T. (2014) Spikar, a novel drebrin-binding protein, regulates the formation and stabilization of dendritic spines. J Neurochem 128(4) 507-22

4. Irie T., Matsuzaki Y., Sekino Y., Hirai H. (2014) Kv3.3 channels harboring a mutation of spinocerebellar ataxia type 13 alter excitability and induce cell death in cultured cerebellar Purkinje cells. J Physiol., 592(Pt1) 229-47

5. Ishikawa M., Shiota J., Ishibashi Y., Hakamata T., Shoji S., Fukuchi M., Tsuda M., Shirao T., Sekino Y., Ohtsuka T., Baraban J.M., Tabuchi A. (2013) Identification, expression and characterization of rat isoforms of the SRF coactivator MKL1. FEBS Open Bio. 3, 387-93

6. Takahashi K., Ishii-Nozawa R., Takeuchi K., Nakazawa K., Sekino Y., Sato K. (2013) Niflumic acid activates additional currents of the human glial L-glutamate transporter EAAT1 in a substrate-dependent manner. Biol Pharm Bull 36(12), 1996-2004

7. Oguchi-Katayama A., Monma A., Sekino Y., Moriguchi T., Sato K. (2013) Comparative gene expression analysis of the amygdalae of juvenile rats exposed to valproic acid at prenatal and postnatal stages. J Toxicol Sci 38(3), 381-402

8. Yamada S., Kotake Y., Sekino Y., Kanda Y. (2013) AMP-activated protein kinase-mediated glucose transport as a novel target of tributyltin in human embryonic carcinoma cells. Metallomics 5:484-91

2. 学会発表

＜国内学会＞

1. 佐藤　薫、関野祐子、化学物質が生後初期神経・グリア新生に及ぼす影響を簡便に検討するための in vitro 評価系の開発、日本薬学会 第 134 年会 (2014. 3) (熊本)
1. 高橋華奈子、最上(重本)由香里、大津香苗、岡田洋平、岡野栄之、関野祐子、佐藤　薫、ヒト iPS 細胞由来神経細胞標本を用いた神経毒性評価系の構築、日本薬学会 第 134 年会 (2014. 3) (熊本)
2. 片山敦子、門馬彰彦、秋友孝文、虞末 愛、星 裕姫乃、守口 徹、関野祐子、佐藤 薫、胎生期および新生期の化学物質暴露の情緒社会性への影響を予測する、遺伝子発現解析に基づく新規評価手法の開発、日本薬学会 第 134 年会 (2014. 3) (熊本)
3. 最上 (重本) 由香里、　千川　和枝、関野　祐子、佐藤　薫、ミクログリアによる血液脳関門の機能制御機構の解明、日本薬学会 第 134 年会 (2014. 3) (熊本)
4. 笠原由香、三浦真理恵、最上 (重本) 由香里、関野祐子、佐藤　薫、鈴木岳之、抗うつ薬と P2X4 受容体の相互作用の比較検討、日本薬学会 第 134 年会 (2014. 3) (熊本)
5. 佐藤　薫、ミクログリアの病理的新機能と生理的新機能—極性からみた神経疾患治療の可能性、第 87 回日本薬理学会年会シンポジウム「ニューロン・グリア連関から紐解く神経疾患」(2014. 3) (仙台)
6. 佐藤　薫、hiPSC-ニューロンで神経特異的有害反応は予測可能か、公開シンポジウム　ヒト iPS 細胞の創薬プロセスへの応用～国際情勢を見据えた新規試験法開発を目指して～ (2014. 2) (東京)
7. Takahashi K, Shigemoto-Mogami Y, Ohtsu K, Okada, Okano H, Sekino Y, Sato K, An attempt to establish the neurotoxicity evaluation system

using human induced pluripotent stem cell-derived neurons, the 7th Takeda science foundation symposium on pharmasciences 'iPS Cells in drug discovery and development' (2013. 1) (大阪)

8. 佐藤　薫、高橋　華奈子、重本一最上　由香里、大津香苗、岡田洋平、岡野栄之、関野祐子、ヒト iPS 細胞由来神経細胞を用いた神経毒性評価系確立の試み、第 22 回日本バイオイメージング学会(2013. 9)(東京)
9. Sato K, Fujimori K, Takaki J, Suzuki T, Sekino Y, P2X4 receptor-mediated acceleration of microglial activation is important for the L-glutamate release from activated microglia in the early stage of inflammation , Neuro2013 (2013. 6) (京都)
10. Shigemoto-Mogami Y, Hoshikawa K, Miura M, Sekino Y, Sato K, Development of in vitro blood-brain barrier model reflecting the function of neurovascular unit, Neuro2013 (2013. 6) (京都)
11. Takahashi K, Irie T, Sekino Y, Sato K, The function of glial excitatory amino-acid transporter EAAT2 is enhanced by docosahexanoic acid, Neuro2013 (2013. 6) (京都)
12. Ohtsu K, Takahashi K, Shigemoto-Mogami Y, Okada Y, Okano H, Sato K, Sekino Y, An Attempt to develop a neurotoxicity evaluation system using human induced pluripotent stem cell-derived neurons vulnerable to exicitotoxicity, Neuro2013 (2013. 6) (京都)
13. Hoshikawa K, Shigemoto-Mogami Y, Ohno Y, Goldman JE, Sekino Y, Sato K, Activated microglia enhance neurogenesis and oligodendrogenesis via inflammatory cytokines, Neuro2013 (2013. 6) (京都)
14. Katayama A, Monma A, Akitomo K, Hirosue M, Hoshi Y, Moriguchi T, Sekino Y, Sato K, Search for genetic markers for the risk of the postnatal exposure to chemical compounds in emotion and social behavior after maturation, Neuro2013 (2013. 6) (京都)
15. 関野祐子、大原由香、佐藤　薫、高橋華奈子、山崎博幸、白尾智明、iPS 細胞由来分化細胞の生理機能を確認するための実験プロトコール作成の試み、第 6 回上肢の神経機能回復セミナー (2013. 6) (秋田)

＜国際学会＞

1. Sato K, Shigemoto-Mogami Y, Goldman JE, Sekino Y, The role of microglia in neurogenesis and oligodendrogenesis in the early postnatal subventricular zone. SfN2013 (2013. 11) (San Diego, USA)
2. Ohara Y, Yamazaki H, Sato K, Shirao T, Sekino Y, Morphological development and expression of synaptic proteins of human iPSC-derived neurons. SfN2013 (2013. 11) (San Diego, USA)
3. Sato K., Takaki J, Fujimori K, Miura M, Suzuki T, Sekino Y, L-Glutamate released from activated microglia down regulates astrocytic L-glutamate transporter expression in neuroinflammation: the 'collusion' hypothesis for increased extracellular L-glutamate concentration in neuroinflammation. ISN-ASN 2013 (2013. 4) (Cancun, Mexico)
4. Sato K, Takaki J, Fujimori K, Miura M, Suzuki T, Sekino Y, L-Glutamate released from activated microglia down regulates astrocytic L-glutamate transporter expression in neuroinflammation. ISN-ASN 2013 satellite meeting (2013. 4) (Merida, Mexico)
5. Sekino Y, Takahashi K, Mogami-Shigemoto Y, Ohtsu K, Okada Y, Okano E, Sato K, Calcium signalling of human iPS-derived neurons responding to ATP and L-glutamate stimulation. ISN-ASN 2013 (2013. 4) (Cancun, Mexico)
6. Sekino Y, Takahashi K, Mogami-Shigemoto Y, Ohtsu K, Okada Y, Okano H, Sato K, Calcium imaging of responses to ATP and L-glutmate stimulation of human iPS-derived neurons. ISN-ASN 2013 satellite meeting (2013. 4) (Playa del Carmen, Mexico)

G. 知的財産権の出願・登録状況

1. 特許取得　　なし
2. 実用新案登録　なし
3. その他　　なし

Figure 1

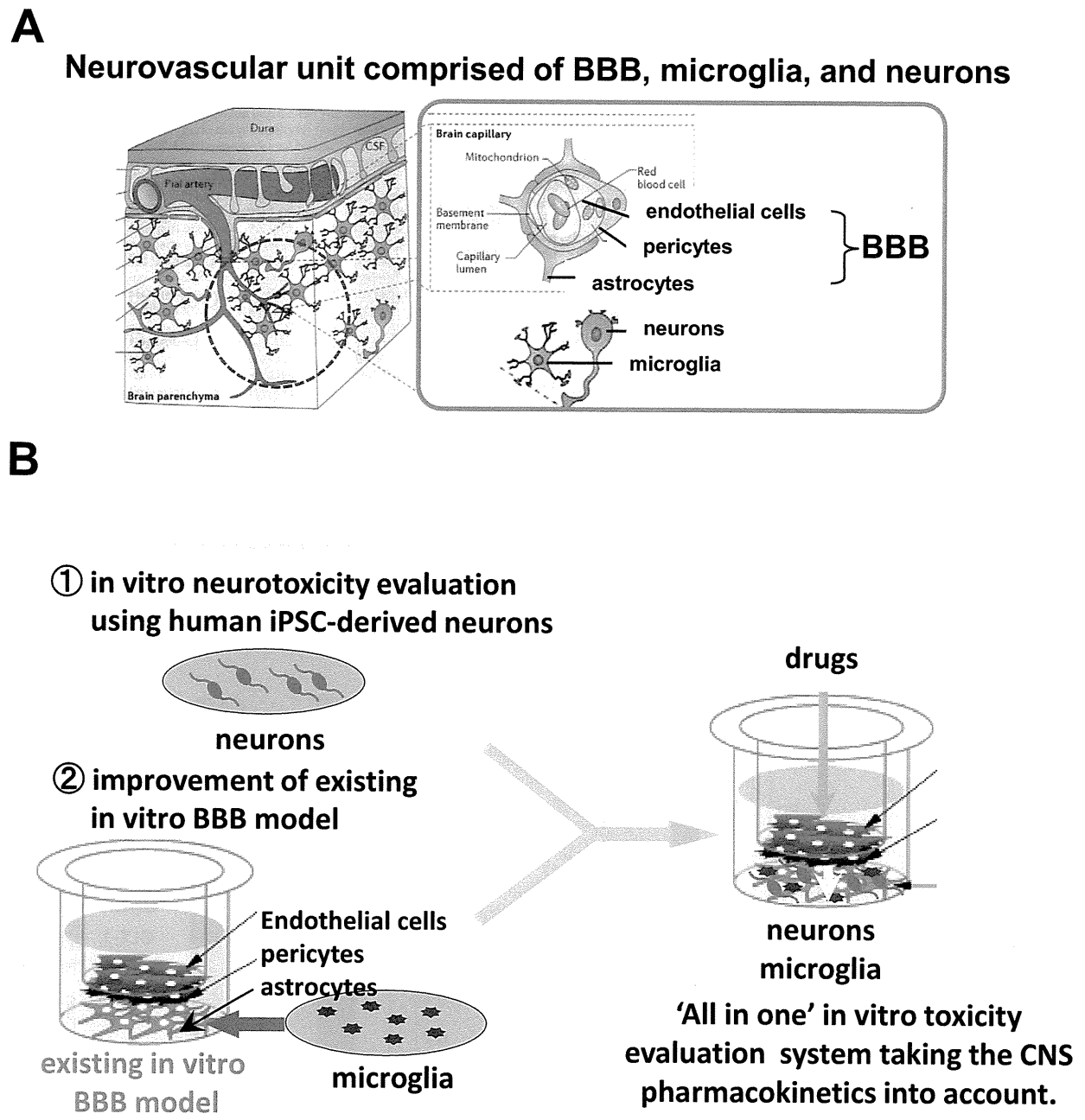

Fig. 1 The concept of our project

A. Neurovascular unit (NVU) is comprised of BBB, microglia, and neurons. Because drugs in the CNS reach neurons via BBB, the model system reproducing NVU is necessary to predict adverse effects on the CNS functions. **B.** We will establish the 'all in one' in vitro toxicity evaluation system taking the CNS pharmacokinetics into account.

Figure 2

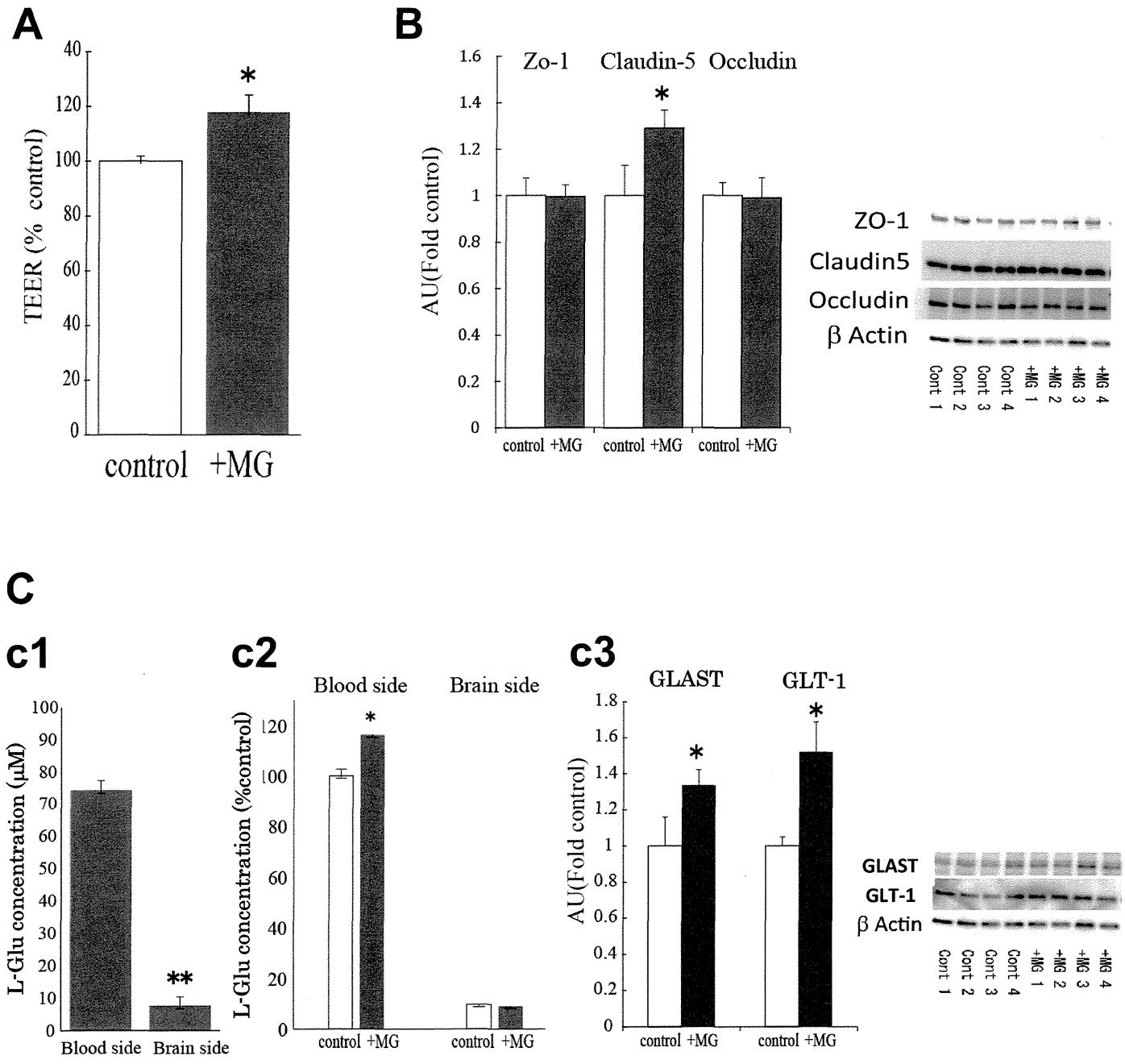

Fig. 2 Effects of microglia on the barrier function of BBB

A. 4-day co-existence of microglia with astrocytes significantly increased TEER of in vitro BBB model. **B.** Microglia also increased the expression level of Claudin5 which is important for the barrier functions of BBB. **C. c1.** After 5 day-incubation, L-Glu (50 μM at the start point) in the brain side was transported to the blood side. **c2.** In the existence of microglia, L-Glu transport from brain side to blood side was significantly enhanced. **c3.** Microglia increased the expression levels of both of GLAST and GLT-1. **: 0.01, *: $p<0.05$, Student's *t* test. Error bars represent s.e.m.

Figure 3

A

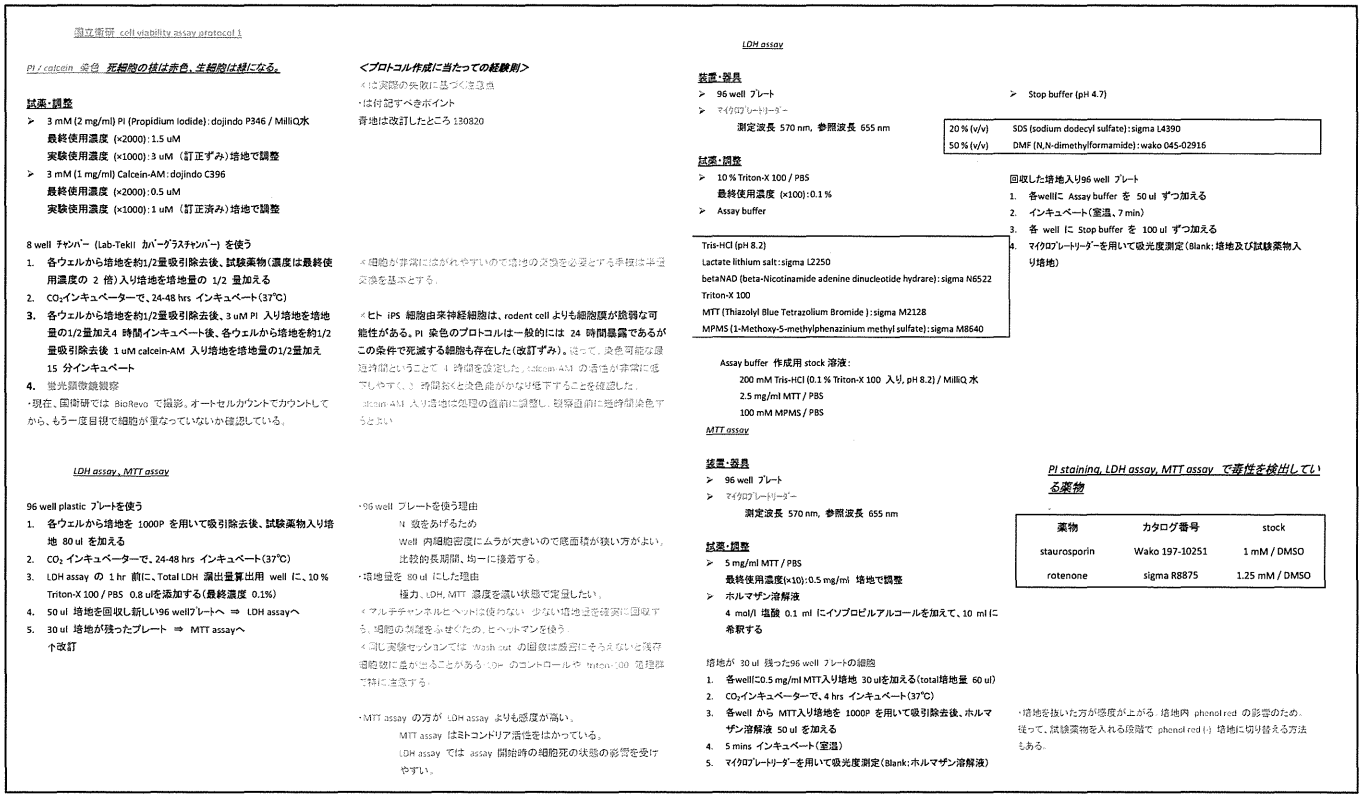

国立衛研 cell viability assay protocol 1

PI / calcein 染色 死細胞の核は赤色、生細胞は緑になる。

試薬・調整

- 3 mM (2 mg/ml) PI (Propidium Iodide): dojindo P346 / MilliQ水
  最終使用濃度 (×2000) : 1.5 uM
  実験使用濃度 (×1000) : 3 uM (訂正ずみ) 培地で調整
- 3 mM (1 mg/ml) Calcein-AM : dojindo C396
  最終使用濃度 (×2000) : 0.5 uM
  実験使用濃度 (×1000) : 1 uM (訂正済み) 培地で調整

8 well チャンバー (Lab-Tekll カバーグラスチャンバー) を使う

1. 各ウェルから培地を約1/2量吸引除去後、試験薬物(濃度は最終使用濃度の 2 倍)入り培地を培地量の 1/2 量加える
2. CO_2インキュベーターで、24-48 hrs インキュベート(37℃)
3. 各ウェルから培地を約1/2量吸引除去後、3 uM PI 入り培地を培地量の1/2量加え4 時間インキュベート後、各ウェルから培地を約1/2量吸引除去後 1 uM calcein-AM 入り培地を培地量の1/2量加え 15 分インキュベート
4. 蛍光顕微鏡観察

・現在、国衛研では BioRevo で撮影。オートセルカウントでカウントしてから、もう一度目視で細胞が重なっていないか確認している。

<プロトコル作成に当たっての経験則>

×は実際の失敗に基づく注意点
・は付記すべきポイント
青地は改訂したところ 130820

×細胞が非常にはがれやすいので培地の交換を必要とする手技は半量交換を基本とする。

×ヒト iPS 細胞由来神経細胞は、rodent cell よりも細胞膜が脆弱な可能性がある。PI 染色のプロトコルは一般的には 24 時間暴露であるがこの条件で死滅する細胞も存在した(改訂ずみ)。従って、染色可能な最短時間ということで 4 時間を設定した。Calcein AM の活性が非常に低下しやすく、3 時間おくと染色能がかなり低下することを確認した。
Calcein AM 入り培地は処理の直前に調整し、観察直前に短時間染色するとよい。

LDH assay、MTT assay

96 well plastic プレートを使う

1. 各ウェルから培地を 1000P を用いて吸引除去後、試験薬物入り培地 80 ul を加える
2. CO_2 インキュベーターで、24-48 hrs インキュベート(37℃)
3. LDH assay の 1 hr 前に、Total LDH 漏出量算出用 well に、10 % Triton-X 100 / PBS 0.8 ulを添加する(最終濃度 0.1%)
4. 50 ul 培地を回収し新しい96 wellプレートへ ⇒ LDH assayへ
5. 30 ul 培地が残ったプレート ⇒ MTT assayへ

十改訂

・96 well プレートを使う理由
  N 数をあげるため
  Well 内細胞密度にムラが大きいので底面積が狭い方がよい。
  比較的長期間、均一に接着する。
・培地量を 80 ul にした理由
  極力、LDH, MTT 濃度を濃い状態で定量したい。

×マルチチャンネルピペットは使わない。少ない培地量を確実に回収する。細胞の剥離をふせぐため、ピペットマンを使う。
×同じ実験セッションでは Wash out の回復は感度にそろえないと残存細胞数に差が出ることがある。DMF のコントロールや Triton-100 処理群で特に注意する。

・MTT assay の方が LDH assay よりも感度が高い。
  MTT assay はミトコンドリア活性をはかっている。
  LDH assay では assay 開始時の細胞死の状態の影響を受けやすい。

LDH assay

装置・器具

- 96 well プレート
- マイクロプレートリーダー
  測定波長 570 nm, 参照波長 655 nm
- Stop buffer (pH 4.7)

20 % (v/v)	SDS (sodium dodecyl sulfate) : sigma L4390
50 % (v/v)	DMF (N,N-dimethylformamide) : wako 045-02916

試薬・調整

- 10 % Triton-X 100 / PBS
  最終使用濃度 (×100) : 0.1 %
- Assay buffer

Tris-HCl (pH 8.2)
Lactate lithium salt : sigma L2250
betaNAD (beta-Nicotinamide adenine dinucleotide hydrate) : sigma N6522
Triton-X 100
MTT (Thiazolyl Blue Tetrazolium Bromide) : sigma M2128
MPMS (1-Methoxy-5-methylphenazinium methyl sulfate) : sigma M8640

Assay buffer 作成用 stock 溶液:
  200 mM Tris-HCl (0.1 % Triton-X 100 入り, pH 8.2) / MilliQ 水
  2.5 mg/ml MTT / PBS
  100 mM MPMS / PBS

回収した培地入り96 well プレート
1. 各wellに Assay buffer を 50 ul ずつ加える
2. インキュベート(室温、7 min)
3. 各 well に Stop buffer を 100 ul ずつ加える
4. マイクロプレートリーダーを用いて吸光度測定(Blank: 培地及び試験薬物入り培地)

MTT assay

装置・器具

- 96 well プレート
- マイクロプレートリーダー
  測定波長 570 nm, 参照波長 655 nm

試薬・調整

- 5 mg/ml MTT / PBS
  最終使用濃度(x10) : 0.5 mg/ml 培地で調整
- ホルマザン溶解液
  4 mol/l 塩酸 0.1 ml にイソプロピルアルコールを加えて、10 ml に希釈する

培地が 30 ul 残った96 well プレートの細胞
1. 各wellに0.5 mg/ml MTT入り培地 30 ulを加える(total培地量 60 ul)
2. CO_2インキュベーターで、4 hrs インキュベート(37℃)
3. 各well から MTT入り培地を 1000P を用いて吸引除去後、ホルマザン溶解液 50 ul を加える
4. 5 mins インキュベート(室温)
5. マイクロプレートリーダーを用いて吸光度測定(Blank: ホルマザン溶解液)

PI staining, LDH assay, MTT assay で毒性を検出している薬物

薬物	カタログ番号	stock
staurosporin	Wako 197-10251	1 mM / DMSO
rotenone	sigma R8875	1.25 mM / DMSO

・培地を扱いた方が感度が上がる 培地内 phenol red の影響のため。従って、試験薬物を入れる段階で phenol red (-) 培地に切り替える方法もある。

B

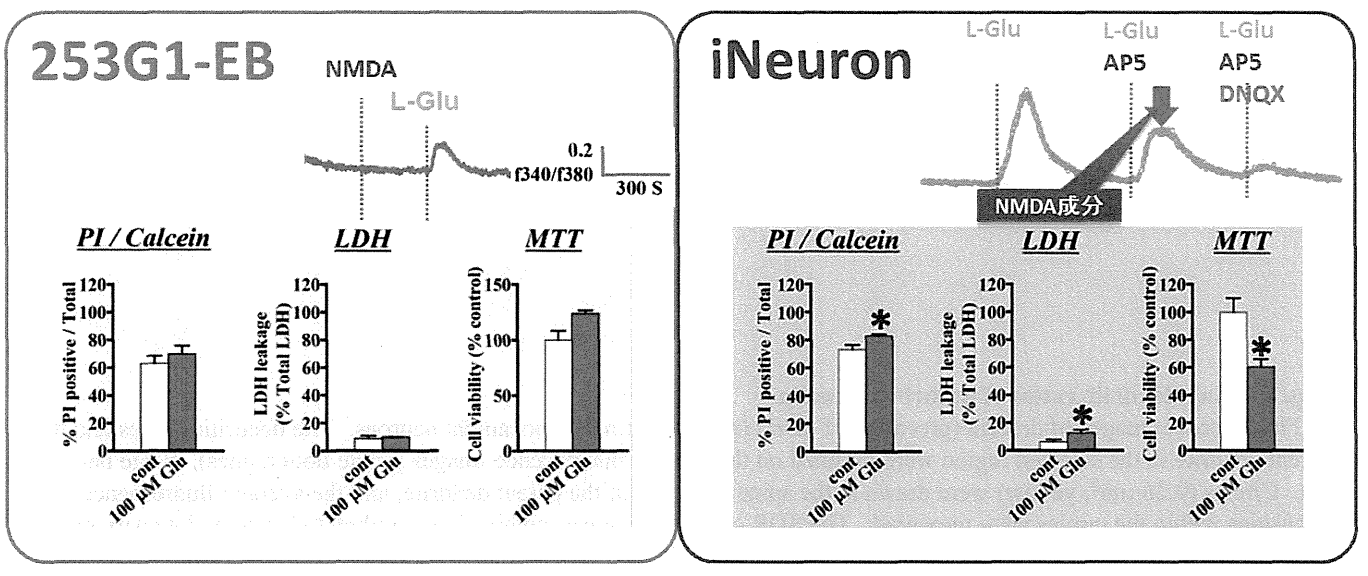

Fig. 3 Establishment of the in vitro toxicity evaluation system using human iPS cell-derived neurons.
A. Protocols of Propidium iodide/calcein staining and LDH/MTT assay optimized for human iPSC-derived neurons. **B.** Evaluation of excitotoxicity using 253G1-derived neurons and iNeurons. L-Glutamate (100 μM, 1 hr) did not cause cell damages to 253G1-derived neurons which had been confirmed not to have NMDA receptors in fura-2 Ca^{2+} imaging, while the same condition caused significant cell damages to iNeurons which had been confirmed to have functional NMDA receptors. n = 6; *: $p<0.05$, Student's *t* test. Error bars represent s.e.m.

Figure 4

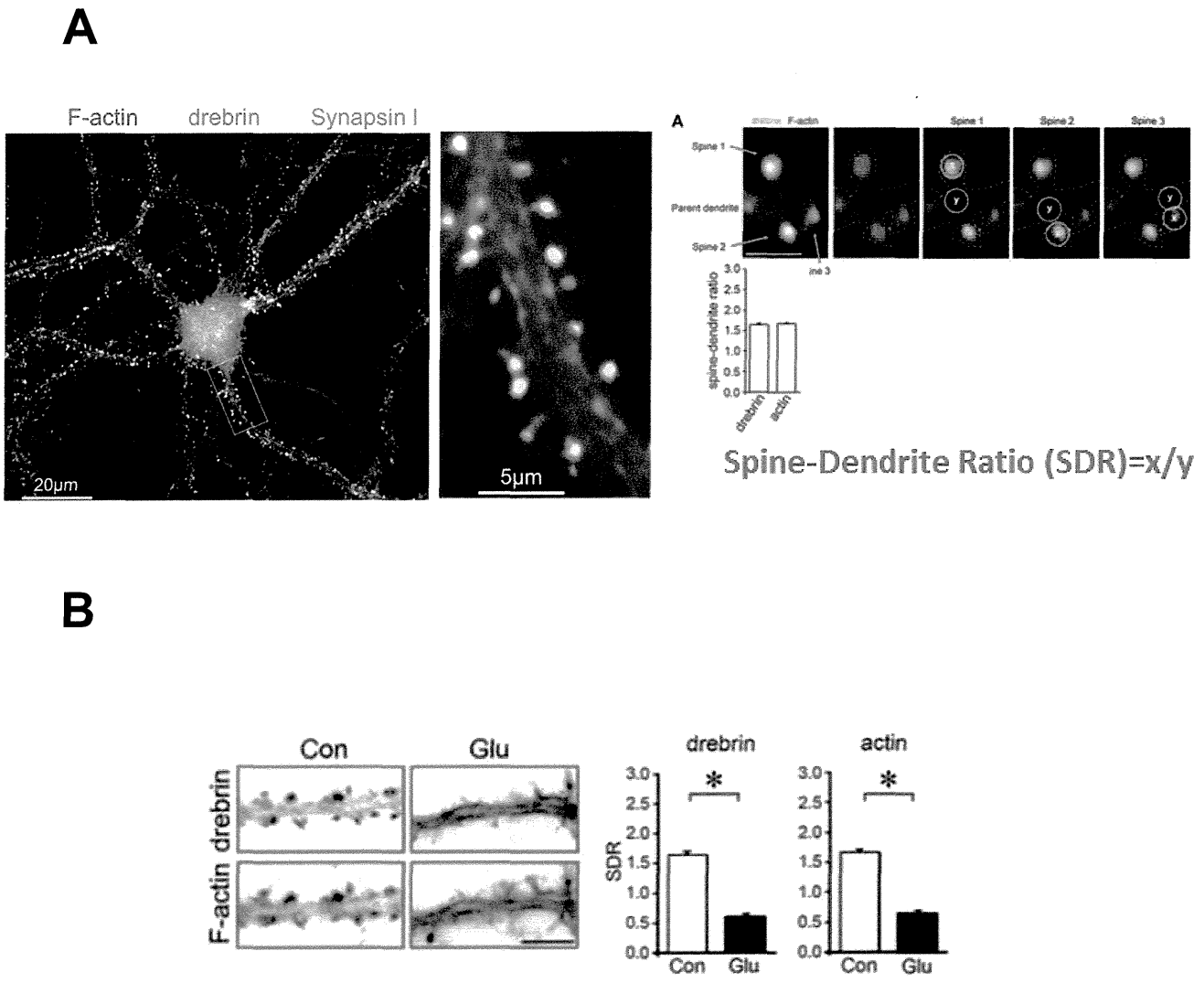

Fig. 4 Spine-dendrite ratios of drebrin and actin

A. Fluorescence images of drebrin (green) and F-actin (red) in control hippocampal neurons. The dendritic spines and the parent dendrite in the selected region were outlined on the F-actin fluorescence images (white dotted lines). Scale bar = 2 μm. Circles (0.26 μm^2, yellow) were drawn at the spine head and at the parent dendrite, and the average fluorescence intensities within the circles were measured. The SDR of each spine was obtained by dividing the average intensity of the dendritic spine by that of the parent dendrite.

B. Effects of L-Glu stimulations (100 μM, 10 min) on drebrin-actin distribution. Images were obtained from neurons (21 DIV) double-labeled for drebrin and F-actin. Bar graphs represent the spine-dendrite ratios (SDRs) for drebrin and actin. After stimulation, the drebrin and F-actin clusters in the spines disappeared, and a linear staining pattern appeared along the dendrite. Both the drebrin and actin SDRs were significantly decreased by L-Glu stimulation. n = 170 cells; *: $p<0.01$, Student's *t* test). Error bars represent s.e.m.

Modified images from Mizui et al., PLOS ONE 9(1) e85367, 2014

別紙４

研究成果の刊行に関する一覧表

書籍

著者氏名	論文タイトル名	書籍全体の編集者名	書　籍　名	出版社名	出版地	出版年	ページ

雑誌

発表者氏名	論文タイトル名	発表誌名	巻号	ページ	出版年
Tashiro K., Nonaka A., Hirata N., Yamaguchi T., Mizuguchi H., **Kawabata K.**	Plasma elevation of vascular endothelial growth factor leads to the reduction of mouse hematopoietic and mesenchymal stem/progenitor cells in the bone marrow.	***Stem Cells Dev.***			in press
Taura A., Furuta K., Yamaguchi T., **Kawabata K.**, Tanaka S.	Regulation of histamine synthesis and tryptase expression through transcription factors, Gfi1 and Gfi1b, in murine cultured mast cells.	***Biol. Pharm. Bull.***	37	81-86	2014
Takayama K., Nagamoto Y., Mimura N., Tashiro K., Sakurai F., Tachibana M., Hayakawa T., **Kawabata K.**, Mizuguchi H.	Long-Term Self-Renewal of Human ES/iPS-Derived Hepatoblast-like Cells on Human Laminin 111-Coated Dishes.	***Stem Cell Reports***	1	322-335	2013
Takayama K., **Kawabata K.**, Inamura M., Ohashi K., Nagamoto Y., Okuno H., Yamaguchi T., Tashiro K., Sakurai F., Hayakawa T., Furue-Kusuda M., Mizuguchi H.	CCAAT/enhancer binding protein-mediated regulation of TGFβ receptor 2 expression determine the hepatoblast fate decision.	***Development***	141	91-100	2014

Yamaguchi T., Tashiro K., Tanaka S., Katayama S., Ishida W., Fukuda K., Fukushima A., Araki R., Abe M., Mizuguchi H., **Kawabata K.**	Two-step differentiation of mast cells from induced pluripotent stem cells.	***Stem Cells Dev.***	22	726-734	2013
Mizui T., **Sekino Y.**, Yamazaki Y., Ishizuka H., Takahashi H., Kojima N., Kojima M., Shirao T.	Myosin II ATPase activity mediates the long-term potentiation-induced exodus of stable F-actin bound by drebrin A from dendritic spines.	***PLOS ONE.***	9(1)	e8536722	2014
Shigemoto-Mogami Y., Hoshikawa K., Goldman J.E., **Sekino Y.**, Sato K.	Microglia enhance neurogenesis and oligodendrogenesis in the early postnatal subventricular zone.	***J Neurosci***	34(5),	2231-2243	2014
Yamazaki H., Kojima N., Kato K., Hirose H., Iwasaki T., Mizui T., Takahashi H., Hanamura K., Roppongi R.T., Koibuchi N., **Sekino Y.**, Mori N., Shirao T.	Spikar, a novel drebrin-binding protein, regulates the formation and stabilization of dendritic spines.	***J Neurochem***	128(4)	507-22	2014
Irie T., Matsuzaki Y., **Sekino Y.**, Hirai H.	Kv3.3 channels harboring a mutation of spinocerebellar ataxia type 13 alter excitability and induce cell death in cultured cerebellar Purkinje cells.	***J Physiol***	592(Pt1) 34	229-47	2014
Ishikawa M., Shiota J., Ishibashi Y., Hakamata T., Shoji S., Fukuchi M., Tsuda M., Shirao T., **Sekino Y.**, Ohtsuka T., Baraban J.M., Tabuchi A.	Identification, expression and characterization of rat isoforms of the SRF coactivator MKL1.	***FEBS Open Bio.***	3	387-93	2013
Takahashi K., Ishii-Nozawa R., Takeuchi K., Nakazawa K., **Sekino Y.**, Sato K.	Niflumic acid activates additional currents of the human glial L-glutamate transporter EAAT1 in a substrate-dependent manner.	***Biol Pharm Bull***	36(12)	1996-2004	2013

Oguchi-Katayama A., Monma A., **Sekino Y.**, Moriguchi T., Sato K.	Comparative gene expression analysis of the amygdalae of juvenile rats exposed to valproic acid at prenatal and postnatal stages.	***J Toxicol Sci***	38(3)	381-402	2013
Yamada S., Kotake Y., **Sekino Y.**, Kanda Y.	AMP-activated protein kinase-mediated glucose transport as a novel target of tributyltin in human embryonic carcinoma cells.	***Metallomics***	5	484-91	2013
山口朋子、**川端健二**	iPS細胞由来マスト細胞を用いた難治性疾患の新規治療薬開発へ向けて	***Biophilia電子版***	2	21-25	2013

STEM CELLS AND DEVELOPMENT
Volume 22, Number 5, 2013

DOI: 10.1089/scd.2012.0339

Two-Step Differentiation of Mast Cells from Induced Pluripotent Stem Cells

Tomoko Yamaguchi,[1] Katsuhisa Tashiro,[1] Satoshi Tanaka,[2] Sumie Katayama,[3] Waka Ishida,[4] Ken Fukuda,[4] Atsuki Fukushima,[4] Ryoko Araki,[5] Masumi Abe,[5] Hiroyuki Mizuguchi,[1,6,7] and Kenji Kawabata[1,6]

Mast cells play important roles in the pathogenesis of allergic diseases. They are generally classified into 2 phenotypically distinct populations: connective tissue-type mast cells (CTMCs) and mucosal-type mast cells (MMCs). The number of mast cells that can be obtained from tissues is limited, making it difficult to study the function of mast cells. Here, we report the generation and characterization of CTMC-like mast cells derived from mouse induced pluripotent stem (iPS) cells. iPS cell-derived mast cells (iPSMCs) were generated by the OP9 coculture method or embryoid body formation method. The number of Safranin O-positive cells, expression levels of CD81 protein and histidine decarboxylase mRNA, and protease activities were elevated in the iPSMCs differentiated by both methods as compared with those in bone marrow-derived mast cells (BMMCs). Electron microscopic analysis revealed that iPSMCs contained more granules than BMMCs. Degranulation was induced in iPSMCs after stimulation with cationic secretagogues or vancomycin. In addition, iPSMCs had the ability to respond to stimulation with the IgE/antigen complex in vitro and in vivo. Moreover, when iPSMCs generated on OP9 cells were cocultured with Swiss 3T3 fibroblasts, protease activities as maturation index were more elevated, demonstrating that mature mast cells were differentiated from iPS cells. iPSMCs can be used as an in vitro model of CTMCs to investigate their functions.

Introduction

MAST CELLS HAVE RECENTLY gained attention, because they have been recognized as effector cells not only in allergic disorders, but also in other immune diseases, including autoimmune diseases and chronic inflammatory disorders [1]. Activation of mast cells triggers allergic and inflammatory responses through the release of a wide variety of mediators, such as histamine, arachidonic acid metabolites, and neutral proteases, and regulates immune responses through the production of cytokines and chemokines [2]. Mast cell precursors leave the bone marrow, migrate in the blood, invade tissues, and then proliferate and differentiate into mature cells [3]. Mature rodent mast cells are generally classified into 2 phenotypically distinct populations: connective tissue-type mast cells (CTMCs) and mucosal-type mast cells (MMCs) [3–4]. Each cell type differs with respect to location, staining characteristics, and histamine content. Mouse CTMCs, which are present in the peritoneal cavity and skin, contain heparin and store large amounts of histamine. In contrast, mouse MMCs, which are prominent in the mucosal layer of the gastrointestinal tract, contain chondroitin sulfate E rather than heparin and have relatively low histamine content. Since recent studies have demonstrated that CTMCs are involved in a wide variety of immune responses [5–7], development of an in vitro culture system of CTMCs is needed. Although several mast cell lines and IL-3-dependent bone marrow-derived mast cells (BMMCs) have been used as models to investigate the process of mast cell activation and subsequent production of proinflammatory mediators, these models have limitations in analyzing the functions specific to mature mast cells. Previous studies showed that coculture of BMMCs with Swiss 3T3 fibroblasts in the presence of stem cell factor (SCF) facilitated morphological and functional maturation toward a CTMC-like phenotype [8].

Differentiation of both mouse and human embryonic stem (ES) cells into multiple hematopoietic lineages is now well established as a powerful tool for studying hematopoietic

[1]Laboratory of Stem Cell Regulation, National Institute of Biomedical Innovation, Osaka, Japan.
[2]Department of Immunobiology, Okayama University Graduate School of Medicine, Dentistry, and Pharmaceutical Sciences, Okayama, Japan.
[3]Bioresources Research, Laboratory of Common Apparatus, National Institute of Biomedical Innovation, Osaka, Japan.
[4]Department of Ophthalmology and Visual Science, Kochi Medical School, Kochi, Japan.
[5]Transcriptome Research Group, National Institute of Radiological Sciences, Chiba, Japan.
[6]Graduate School of Pharmaceutical Sciences, Osaka University, Osaka, Japan.
[7]The Center for Advanced Medical Engineering and Informatics, Osaka University, Osaka, Japan.

differentiation and lineage restriction, and for generating unlimited numbers of hematopoietic stem and progenitor cell populations for transplantation [9–12]. ES or induced pluripotent stem (iPS) cells into hematopoietic cells have been differentiated by embryoid body (EB) formation or coculture with stromal cells, such as OP9 cells [13–16]. By using these protocols, several groups have previously established methods to generate mast cells from mouse [17–19], cynomolgus monkey [20], and human [21] ES cells. ES cell-derived mast cells could respond to stimulation with antigen and substance P by releasing histamine. However, in most cases, these cells do not develop the large granules and high levels of proteolytic enzymes characteristic of tissue mast cells.

In this study, we generated mast cells from mouse iPS cells (iPSMCs), and characterized them from the point of view of morphology, function, and gene expression. Our results showed that the iPSMCs that were differentiated by coculture with OP9 stromal cells or the EB formation method had characteristics similar to CTMCs. When iPSMCs that were generated on OP9 cells were cocultured with Swiss 3T3 fibroblasts, the iPSMCs exhibited a more functional phenotype.

Materials and Methods

Cell cultures

Two mouse iPS cell clones, 38C2 (a kind gift from Dr. S. Yamanaka, Kyoto University, Kyoto, Japan) [22] and 2A-EGFPTg-4F-01 [23], were used in the present study. These mouse iPS cells were routinely cultured in a leukemia inhibitory factor-containing ES cell medium (Specialty Media) on mytomycin C-treated mouse embryonic fibroblasts (MEFs; Specialty Media), and they were passaged every 2 days using 0.25% trypsin-EDTA (Invitrogen). OP9 stromal cells were cultured in an α-minimum essential medium (α-MEM: Sigma) supplemented with 20% fetal bovine serum (FBS), 2 mM L-glutamine (Invitrogen), and 1×nonessential amino acid (NEAA; Invitrogen).

Generation of BMMCs

C57BL/6 mice were purchased from Nippon SLC. Bone marrow cells were prepared from the femurs and tibiae of mice. Cells were cultured in an RPMI 1640 medium containing 10% FBS, 1×NEAA, and 10 ng/mL murine IL-3 (R&D Systems). The culture medium was replaced with a fresh medium every 5 days. After 4 weeks of culture, we confirmed the cellular surface expression of both FcεRI and c-kit (>95% positive).

Differentiation of iPS cells to mast cells

Before coculturing with OP9 cells or EB formation, mouse iPS cells were suspended in an ES cell medium and cultured on a culture dish at 37°C for 30 min to remove MEF layers. In the OP9 cell-mediated differentiation method, iPS cells were transferred onto OP9 cells in 6-well plates at a density of 1×10^4 cells per well. The induced cells were trypsinized on day 7, and 1×10^5 cells were seeded onto fresh OP9 cells with α-MEM supplemented with 20% FBS, 2 mM L-glutamine, 1×NEAA, 30 ng/mL IL-3, and 100 ng/mL SCF (Peprotech). After 7 days, nonadherent cells were reseeded onto fresh OP9 cells. The cells were subcultured every 7 days. We harvested the differentiated cells on day 28 and used them for further analysis.

In the EB-mediated differentiation method, iPS cell-derived EBs were generated by culturing iPS cells on a round-bottom low-cell-binding 96-well plate at 1×10^3 cells per well. iPS cell-derived EBs were collected on day 7, and were transferred to a Petri dish with Differentiation Medium I [Dulbecco's modified Eagle's medium containing 15% FBS, 1×NEAA, 2 mM L-glutamine, 1×nucleosides, 0.1 mM 2-mercaptoethanol, penicillin/streptomycin, 30 ng/mL IL-3, 30 ng/mL IL-6 (Peprotech), and 100 ng/mL SCF]. After 7 days, nonadherent cells were transferred to a culture dish with Differentiation Medium II (Dulbecco's modified Eagle's medium containing 10% FBS, 1×NEAA, 2 mM L-glutamine, penicillin/streptomycin, 30 ng/mL IL-3, and 100 ng/mL SCF). We harvested the nonadherent cells on day 28 and used them for further analysis.

Transmission electron microscopy

BMMCs or iPSMCs were fixed with 2.5% glutaraldehyde in 0.1 M sodium phosphate buffer (pH 7.4), postfixed with 1% OsO_4, dehydrated by a graded ethanol series, passed through QY-1 (Nisshin EM), and then embedded in Epon-812 (TAAB,). Ultrathin sections (0.06-μm thick) were cut with an ultramicrotome (Leica Microsystems), stained with uranyl acetate–lead citrate, and observed using an electron microscope (H-7650, HITACHI) at 80 kV.

Protease assay

BMMCs or iPSMCs were washed with phosphate-buffered saline (PBS), lysed in PBS containing 2 M NaCl/0.5% Triton X-100, and incubated for 30 min on ice. The lysate was centrifuged at 12,000 rpm for 30 min at 4°C. Activities of granule proteases in the resultant supernatants were measured using their specific chromogenic peptide substrates, such as S-2288 for tryptase (Sekisui medical) and M-2245 for carboxypeptidase A (CPA; Bachem) [24].

β-hexosaminidase release assay

β-hexosaminidase activity was measured as a marker of the granular fraction for evaluation of degranulation. Cells were washed with an HEPES buffer (137 mM NaCl, 20 mM HEPES, 5 mM D-glucose, 2.7 mM KCl, 0.4 mM NaH_2PO_4, 0.5 mM $MgCl_2$, 2.4 mM $CaCl_2$, and 0.1% bovine serum albumin) and incubated with the buffer containing compound 48/80 (10 μg/mL; Sigma) or substance P (100 μM; Sigma) for 30 min. In the case of antigen stimulation, mast cells sensitized with 1 μg/mL anti-dinitrophenyl (DNP) IgE (SPE7; Sigma-Aldrich) for 24 h were stimulated with 100 ng/mL DNP-human serum albumin (HSA; Biosearch Technologies) in the presence of lysophosphatidylserine (Lyso-PS; Avanti Polar Lipids).

Coculture of mast cells with Swiss 3T3 fibroblasts

iPSMCs obtained after 28 days of culture with OP9 cells were cocultured with mitomycin C-treated Swiss 3T3 fibroblasts in the presence of 100 ng/mL SCF. BMMCs were

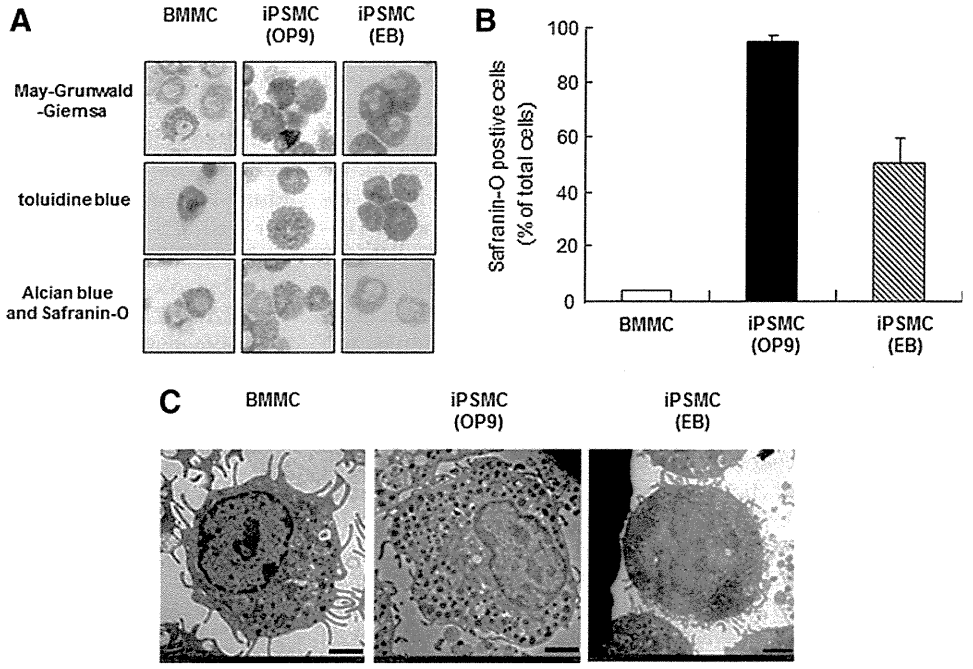

FIG. 1. Morphological characterization of induced pluripotent stem cell-derived mast cells (iPSMCs). **(A)** The iPSMCs, which were differentiated by coculture with OP9 cells or the embryoid body formation method, were harvested on day 28. Cytocentrifuged preparations of bone marrow-derived mast cells (BMMCs) and the iPSMCs were stained with May-Grunwald-Giemsa, toluidine blue, or Alcian blue and Safranin O solutions. **(B)** The ratio of Safranin O-positive cells to total cells was calculated and shown as a percentage. The data represent the means ± S.D. ($n=4$). **(C)** BMMCs and iPSMCs were visualized by transmission electron microscopy. Scale bar = 2.0 μm.

also cocultured with Swiss 3T3 fibroblasts under the same conditions. The subculture was performed every 4 days. The cells were trypsinized and replated, and nonadherent cells were collected as mast cells and used for further analysis.

Mast cell reconstitution and induction of passive cutaneous anaphylaxis

BMMCs or iPSMCs (5×10^5 cells) were injected subcutaneously into the conjunctivae of mast cell-deficient $Kit^{W\text{-}sh/W\text{-}sh}$

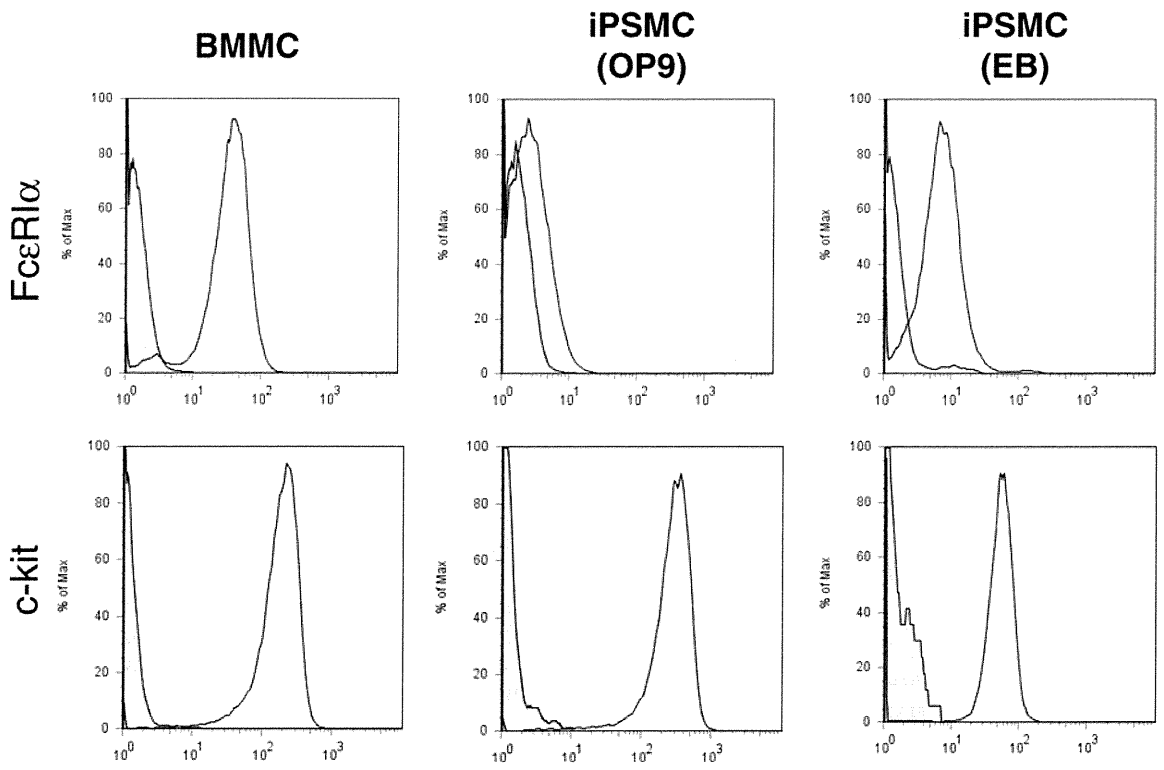

FIG. 2. Flow cytometric analysis of FcεRI and c-kit expression on iPSMCs. BMMCs and iPSMCs were stained with FITC-labeled anti-FcεRI and PE-labeled anti-c-kit antibodies for 30 min on ice. Stained cells were washed, resuspended in 1% fetal bovine serum–phosphate-buffered saline (FBS-PBS), and analyzed by flow cytometry.

mice. To elicit passive cutaneous anaphylaxis reactions, mice were injected subcutaneously into the conjunctiva with 75 ng anti-DNP IgE or saline. Then, 24 h after IgE injection, 100 μg DNP-HSA containing 2% Evan's blue dye was injected intravenously into mice. Thirty minutes later, the mice were killed, and their conjunctivae were excised. Evan's blue dye was extracted from conjunctivae with formamide, and the absorbance was measured at 610 nm.

Results

Generation of mast cells from mouse iPS cells

iPSMCs were generated by the OP9 coculture method or EB formation method as described in Supplementary Fig. S1 (Supplementary Data are available online at www.liebertpub.com/scd). Approximately 6.5×10^6 mast cells could be obtained from 1×10^5 iPS cells by coculturing them with OP9 cells for 4 weeks. In addition, as in the case of BMMCs, iPSMCs can retain their proliferative potential (data not shown).

Next, we performed the staining with May-Grunwald-Giemsa, toluidine blue, Alcian blue, and Safranin O solutions. May-Grunwald-Giemsa staining of the iPSMCs, which were differentiated by coculture with OP9 stromal cells or the EB formation method (Supplementary Fig. S1), revealed that induced mast cells gave rise to a uniform phenotype with rough basophilic granule-containing cells (Fig. 1A, upper). The granules in these cells showed a metachromatic staining pattern when stained with acid toluidine blue (Fig. 1A, middle). We then performed Alcian blue and Safranin O staining, by which mast cells are known to show a specific red color if they are CTMCs and a blue color if they are immature mast cells or MMCs [1]. While BMMCs were Alcian blue positive and Safranin O negative, iPSMCs were positive for both Alcian blue and Safranin O staining (Fig. 1A, [lower], B). Electron microscopic analysis revealed that the iPSMCs differentiated by either method contained more granules than BMMCs (Fig. 1C).

Expression of high-affinity IgE receptor on iPSMCs

Mast cells are known to express c-kit and FcεRI (high-affinity IgE receptor) [1]. We next performed flow cytometric analysis to examine the surface expression of c-kit and FcεRI on iPSMCs. There was no significant difference in c-kit expression levels between iPSMCs and BMMCs (Fig. 2). In contrast, the FcεRIα expression level was significantly lower in the iPSMCs that were generated by coculture with OP9 cells, compared with that in BMMCs. Both c-kit$^+$FcεRI$^+$ and c-kit$^+$FcεRI$^-$ cells showed a granular phenotype by forward and side scatter (data not shown).

FcεRI is a heterotrimer composed of one α-chain and 2 γ-chains or a heterotetramer composed of one β-chain and 2 γ-chains. To evaluate the expression of each FcεRI subunit in iPSMCs, we analyzed mRNA expression levels by reverse transcription and quantitative polymerase chain reaction (RT-PCR). As shown in Supplementary Fig. S2, the expression levels of the mRNAs encoding the FcεRIα, FcεRIβ, and FcεRIγ chains were reduced in the iPSMCs differentiated by either method as compared with the levels in BMMCs.

Phenotypic differences between iPSMCs and BMMCs

To further compare the degree of mast cell differentiation, we measured the tryptase and CPA activities in iPSMCs. The tryptase and CPA activities were elevated in the iPSMCs derived from either method as compared with those in BMMCs (Fig. 3).

Histidine decarboxylase (HDC) is a critical enzyme that is involved in the synthesis of endogenous histamine in mammals [25–26], and is considered to be one of the indices of mast cell maturation [26]. Therefore, quantitative RT-PCR analysis was performed to compare the expression of HDC mRNA levels in iPSMCs and BMMCs (Supplementary Fig. S3). The expression level of HDC mRNA was elevated in the iPSMCs that were differentiated by either method as compared with that in BMMCs.

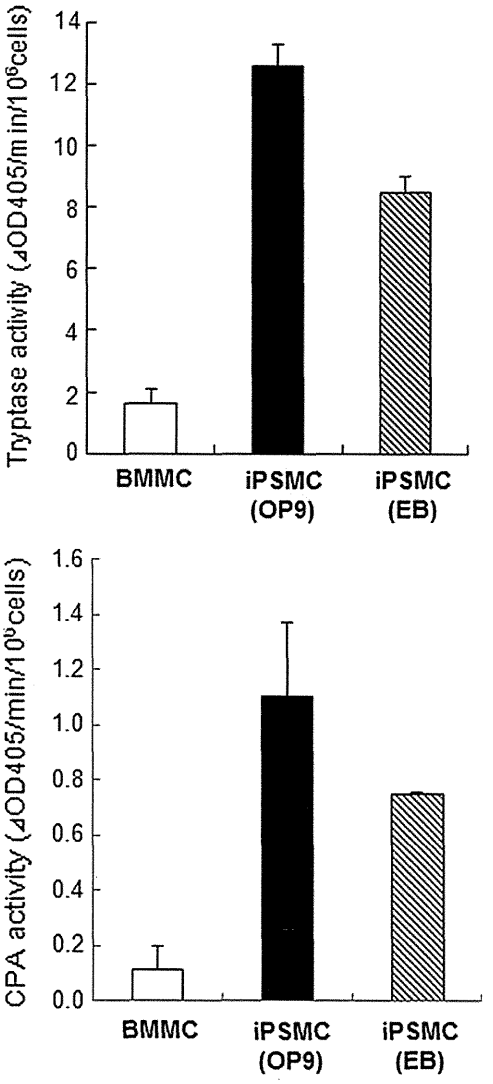

FIG. 3. Tryptase and carboxypeptidase A (CPA) activities in iPSMCs. Cell extracts prepared from BMMCs and iPSMCs were assayed for tryptase and CPA activities as described in the Materials and Methods section. All data represent the means ± S.D. ($n=4$).

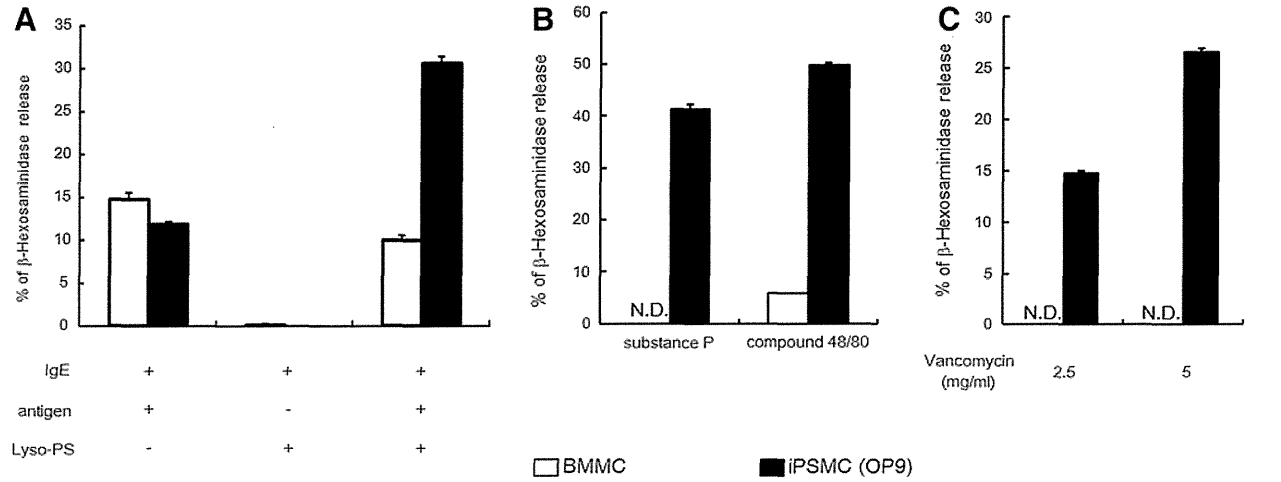

FIG. 4. β-hexosaminidase release from iPSMCs after stimulation with IgE/antigen, compound 48/80, substance P, and vancomycin. **(A)** The exocytotic response was determined by measuring the release of β-hexosaminidase. BMMCs (*open bar*) and the iPSMCs that were cocultured with OP9 cells (*closed bar*) were sensitized with anti-dinitrophenyl (DNP) IgE and stimulated with DNP human serum albumin (HSA) in the presence or absence of Lyso-PS as described in the Materials and Methods section. β-hexosaminidase enzymatic activity was measured in supernatants and cell pellets solubilized with 0.5% Triton X-100 in HEPES buffer. **(B)** BMMCs (*open bar*) and the iPSMCs that were cocultured with OP9 cells (*closed bar*) were stimulated with compound 48/80 or substance P. **(C)** BMMCs (*open bar*) and the iPSMCs that were cocultured with OP9 cells (*closed bar*) were stimulated with vancomycin. All data represent the means ± S.D. ($n = 3$).

Previously, Takano *et al.* demonstrated that *CD81*, a member of the tetraspanin superfamily, is one of the strikingly upregulated genes in BMMCs cocultured with Swiss 3T3 fibroblasts [8]. CD81 is also considered to be a marker of CTMCs. FACS analysis showed that expression of CD81 was elevated in the iPSMCs differentiated by either method as compared with that in BMMCs (Supplementary Fig. S4). In particular, our results revealed that the iPSMCs that were differentiated by coculture with OP9 cells were almost all CD81 positive and showed a homogeneous population.

Degranulation of iPSMCs

We compared FcεRI-mediated degranulation of BMMCs and iPSMCs by measuring the extracellular activity of β-hexosaminidase, a marker enzyme for histamine-containing granules. As shown in Fig. 4A, the iPSMCs that were differentiated by coculture with OP9 cells displayed significantly less release of β-hexosaminidase than the BMMCs in response to IgE-mediated antigen stimulation. Similar results were obtained in iPSMCs that were derived from EB formation methods (Supplementary Fig. S5A). On the other hand, when the iPSMCs that were pretreated with anti-DNP monoclonal IgE were incubated with DNP-HSA in the presence of Lyso-PS, which is known to enhance IgE-mediated degranulation in rat peritoneal mast cells [27], the amount of β-hexosaminidase release was increased.

Responses to cationic secretagogues such as compound 48/80 and substance P are functional characteristics of CTMCs [4]. We next compared the IgE-independent responses between BMMCs and iPSMCs. Stimulation of iPSMCs with compound 48/80 resulted in marked exocytosis of β-hexosaminidase, whereas no or little release of this enzyme was detected from stimulated BMMCs (Fig. 4B and Supplementary Fig. S5B). Similarly, β-hexosaminidase release from iPSMCs was much more markedly elevated by substance P treatment than β-hexosaminidase release from BMMCs (Fig. 4B and Supplementary Fig. S5B). In addition, stimulation of iPSMCs with vancomycin resulted in marked exocytosis of β-hexosaminidase, whereas no or little release of β-hexosaminidase was detected from vancomycin-stimulated BMMCs (Fig. 4C and Supplementary Fig. S5C). These results indicate that the iPSMCs display a CTMC-like phenotype.

Comparison between iPSMCs differentiated by the OP9 coculture and EB formation protocols

We next compared the degree of differentiation between the iPSMCs that were differentiated by the OP9 coculture method and those differentiated by the EB formation method. The expression level of FcεRI was significantly lower in the iPSMCs that were differentiated by coculture with OP9 cells as compared with the iPSMCs that were differentiated by EB formation (Fig. 2). However, the number of Safranin O-positive cells was significantly greater in the iPSMCs that were cocultured with OP9 cells than in the iPSMCs that were derived from the EB formation method (Fig. 1B). In addition, the expression levels of HDC mRNA and CD81 protein were significantly higher in the iPSMCs that were cocultured with OP9 cells than in those that were derived from the EB formation method (Supplementary Figs. S3 and S4). These results showed that the iPSMCs that were cocultured with OP9 cells were more mature than the iPSMCs that were derived from the EB formation method. The iPSMCs that were derived from EB formation were more mature than BMMCs (Figs. 1–3). During the differentiation step, the iPSMCs that were derived from the EB formation method were designated as mast cells I (Fig. 5F). The iPSMCs that were differentiated by coculture with OP9 cells were also designated as mast cells II.

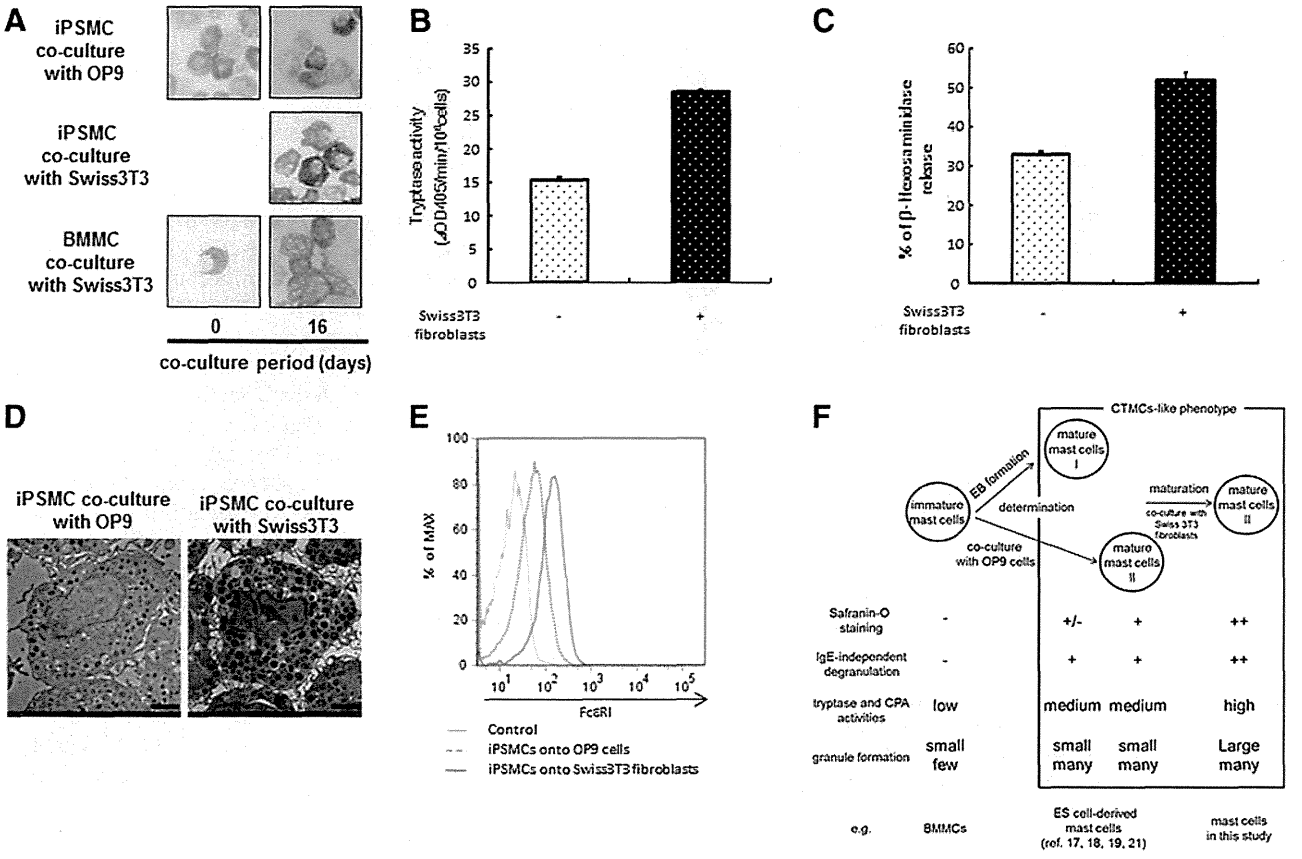

FIG. 5. Maturation of iPSMCs cocultured with Swiss 3T3 fibroblasts in the presence of stem cell factor. **(A)** Cytocentrifuged preparations of the iPSMCs that were cocultured with OP9 cells or Swiss 3T3 fibroblasts, and the BMMCs that were cocultured with Swiss 3T3 fibroblasts were stained with Alcian blue and Safranin O. **(B)** Granule protease activities of the iPSMCs that were cocultured with OP9 cells or Swiss 3T3 fibroblasts were measured. **(C)** The exocytotic response was determined by measuring the release of β-hexosaminidase. The iPSMCs that were cocultured with OP9 cells (*open bar*) or Swiss 3T3 fibroblasts (*closed bar*) were stimulated with compound 48/80. **(D)** The iPSMCs that were cocultured with OP9 cells or Swiss 3T3 fibroblasts were analyzed by transmission electron microscopy. Scale bar = 2.0 μm. **(E)** Suspensions of the iPSMCs that were cocultured with OP9 cells or Swiss 3T3 fibroblasts were stained with FITC-labeled anti-FcεRI antibody for 45 min on ice. The stained cells were washed, resuspended in 1% FBS-PBS, and analyzed by flow cytometry. **(F)** Scheme of 2-step differentiation of mast cells from iPS cells. All data represent the means ± S.D. ($n = 3$).

Enhancement of maturation in iPSMCs by Swiss 3T3 fibroblasts

A previous study reported that coculture of BMMCs with Swiss 3T3 fibroblasts in the presence of SCF facilitated morphological and functional maturation toward a CTMC-like phenotype [8]. It is possible that Swiss 3T3 fibroblasts promote the maturation of the iPSMCs (mast cells II) that are generated on OP9 cells. Therefore, we expected to generate more mature iPSMCs by coculturing with Swiss 3T3 fibroblasts. We compared the degree of mast cell maturation of the iPSMCs that were cocultured with OP9 cells or Swiss 3T3 fibroblasts. Although the majority of BMMCs were Alcian blue positive and Safranin O negative, the percentage of Safranin O-positive mast cells was gradually increased up to ~80% on day 16 after coculturing with Swiss 3T3 fibroblasts (Fig. 5A). The staining intensity for Safranin O on the iPSMCs that were cocultured with Swiss 3T3 fibroblasts was stronger than the iPSMCs (mast cells II) (Fig. 5A). Therefore, the iPSMCs that were differentiated by coculture with Swiss 3T3 fibroblasts were found to be more mature than mast cells II and designated as mast cells III (Fig. 5F). We measured the tryptase activity in the iPSMCs (mast cells II) or iPSMCs (mast cells III), and found the elevated tryptase activity in the iPSMCs (mast cells III) relative to the iPSMCs (mast cells II) (Fig. 5B). Similarly, β-hexosaminidase release by compound 48/80 in the iPSMCs (mast cells III) was markedly elevated in comparison with that in the iPSMCs (mast cells II) (Fig. 5C). Electron microscopic analysis of mast cells revealed that the iPSMCs (mast cells III) contained more large granules (Fig. 5D). We performed flow cytometric analysis to examine the surface expression of c-kit and FcεRI on the iPSMCs (mast cells III). After coculturing, iPSMCs (mast cells III) and BMMCs still expressed similar levels of c-kit (data not shown). Remarkably, the expression level of FcεRI was elevated in the iPSMCs (mast cells III) (Fig. 5E). These results showed that there were 2 steps in iPSMC maturation process.

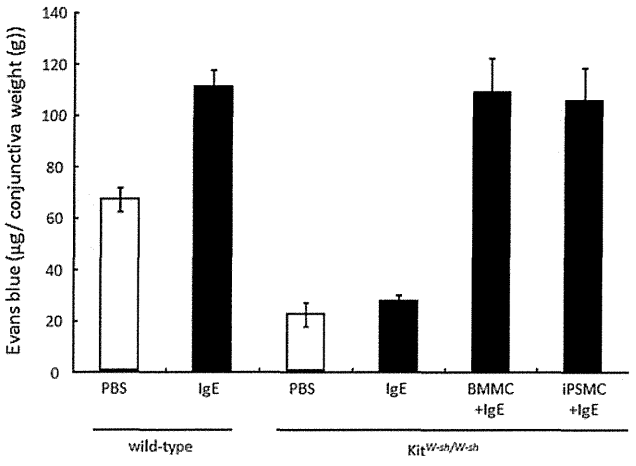

FIG. 6. IgE-dependent passive cutaneous anaphylaxis in mast cell-deficient $Kit^{W\text{-}sh/W\text{-}sh}$ mice reconstituted with iPSMCs. BMMCs or iPSMCs were injected subcutaneously into the conjunctivae of mast cell-deficient $Kit^{W\text{-}sh/W\text{-}sh}$ mice. After 6 weeks, mice were subcutaneously sensitized with anti-DNP IgE or saline, followed by induction of passive cutaneous anaphylaxis. After 24 h, mice were intravenously injected with DNP-HSA along with 2% Evan's blue dye. Thirty minutes later, conjunctivae were excised, and Evan's blue dye was extracted. Extravasation of Evan's blue dye was quantified as described in the Materials and Methods section. Results are normalized to average conjunctivae weight and are expressed as mean ± S.D. ($n = 3$ mice per group).

Mast cell reconstitution and induction of passive cutaneous anaphylaxis

We assessed whether the iPSMCs (mast cells I) with a C57BL/6 background could exhibit passive cutaneous anaphylaxis 6 weeks after injection of iPSMCs or BMMCs into the conjunctiva of mast-cell-deficient ($Kit^{W\text{-}sh/W\text{-}sh}$) mice [28]. $Kit^{W\text{-}sh/W\text{-}sh}$ mice reconstituted with BMMCs or iPSMCs exhibited passive cutaneous anaphylaxis reactions in the conjunctivae as measured by extravasation of Evan's Blue dye (Fig. 6). On the other hand, no passive cutaneous anaphylaxis reactions in the conjunctivae were observed for $Kit^{W\text{-}sh/W\text{-}sh}$ mice that were not reconstituted with mast cells. These results indicate that iPSMCs had the ability to respond to stimulation with IgE/antigen in vivo.

Discussion

In this study, we developed a protocol consisting of mesoderm induction (stage 1), mast cell specification (stage 2), determination of mast cells (stage 3), and maturation of mast cells (stage 4) for mast cell differentiation from iPS cells (Supplementary Figs. S1 and S6). BMMCs have been used extensively as a mast cell model. We compared the degree of maturation in BMMCs and iPSMCs. Expression level of CD81 was higher in the iPSMCs that were differentiated by both methods than in BMMCs (Supplementary Fig. S4). We also showed that IgE-mediated degranulation of iPSMCs was elevated in comparison with that in BMMCs in the presence of Lyso-PS (Fig. 4A and Supplementary Fig. S5A), demonstrating that iPSMCs were more mature than BMMCs. Therefore, both OP9 cells and EB-derived feeder cells might moderately promote the maturation of mast cells. The other possibility is that the maturation of iPSMCs might be accelerated by SCF. SCF is one of the most important cytokines for mast cell maturation [29]. BMMCs are in general generated without SCF. These are reasons why iPSMCs were more mature than BMMCs with respect to their phenotypes and functions.

Cytokines and feeder cells were required to induce the mast cell development from mouse iPS cells. As previously described, IL-3 is known to play an important role in mast cell specification. In contrast, BMMCs are generated without OP9 cells, suggesting that OP9 cells are not necessary for mast cell specification. OP9 cells might promote the maturation of mast cells, possibly by OP9 cell-derived factors, such as IL-4 [30–31], IL-6 [32–34], and nerve growth factor [34]. Therefore, cytokines and OP9 cells are all-essential and have distinct roles in the differentiation of mast cells from iPS cells.

We found a difference in FcεRI expression levels between iPSMCs (mast cell I) and iPSMCs (mast cell II) (Fig. 2). Surface expression level of FcεRI was lower in the iPSMCs (mast cells II), compared with that in the iPSMCs (mast cells I). More recently, Kovarova *et al.* reported that expression of FcεRIα mRNA was lower in human ES cell-derived mast cells that were cocultured with OP9 cells than in human ES cell-derived mast cells that were derived from the EB formation method [21]. These findings were fully consistent with our results. However, our results showed that iPSMCs (mast cells II) were more mature than iPSMCs (mast cells I). These results indicate that the expression levels of FcεRI are not completely correlated with the degree of mast cell differentiation, although the iPSMCs (mast cells III) showed a high level of FcεRI expression (Fig. 5E).

In the present study, we demonstrated that, as in the case of BMMCs, Swiss 3T3 fibroblasts could promote the maturation of iPSMCs (Fig. 5). A recent study has reported that cynomolgus monkey ES cells that are cocultured with the murine aorta-gonad-mesonephros-derived stromal cell line AGM-S1 cells are differentiated into CTMCs [20]. These results suggest that feeder cells, including AGM-S1 and Swiss3T3 fibroblasts, would promote mast cell maturation by similar mechanisms. These feeder cells might contribute to the identification of factors that play a role in mast cell maturation.

While iPSMCs (mast cells II) were almost all Safranin O positive, iPSMCs (mast cells I) included both Safranin O-positive and negative populations, suggesting that immature cells were contained in iPSMCs (mast cells I). Expression levels of CD81 protein and HDC mRNA, and protease activities, were slightly elevated in the iPSMCs (mast cells II) as compared with the iPSMCs (mast cells I). Our results suggest that the iPSMCs (mast cells II) were more mature than iPSMCs (mast cell I). The iPSMCs (mast cells III) exhibited more mature phenotypes, such as large granules and high activity of protease. Taken together, the rank order of maturity in mast cells was the following: iPSMCs (mast cells III) > iPSMCs (mast cells II) > iPSMCs (mast cells I). The precise mechanisms of mast cell maturation process remain to be clarified. Classification of mast cells by using cell surface or internal marker can contribute to clarify the maturation mechanism of mast cells. Further studies are needed to find cell surface or internal marker that can clearly distinguish iPSMCs (mast cells I and II) and iPSMCs (mast cells III).

Our data demonstrate that iPSMCs could functionally respond to IgE stimulation in vivo (Fig. 6). There was no significant difference in Evan's blue extravasation in the $Kit^{W\text{-}sh/W\text{-}sh}$ mice reconstituted with iPSMCs or BMMCs. Previously, Fukuda *et al.* demonstrated that conjunctiva reconstituted with BMMCs display a CTMC-like phenotype [28]. Therefore, passive cutaneous anaphylaxis reactions were comparable in $Kit^{W\text{-}sh/W\text{-}sh}$ mice reconstituted with iPSMCs or BMMCs.

Galli's group first reported the identification of mast cell-committed progenitors (MCPs) in adult murine bone marrow [35]. They indicated that MCPs may be directly developed from multipotential progenitors independent of the myeloid pathway. In contrast, Arinobu *et al.* demonstrated that granulocyte/monocyte progenitors gave rise to MCPs [36]. The models of the developmental process in mast cells differed between these 2 reports. To analyze cells at each differentiation step, our differentiation protocol will be useful for clarifying the developmental process of mast cells.

Because of their pluripotency and self-renewal, ES cells and iPS cells are potential cell sources for regenerative medicine and other clinical applications, such as cell therapies, drug screening, toxicology, and investigation of disease mechanisms. Notably, iPS cell-based screening approaches might support the development of personalized medicine and tailor-made treatment plans. Vancomycin, an antibiotic to which methicillin-resistant *Staphylococcus aureus* (MRSA) is sensitive, frequently induces allergic reaction [37]. In this study, the stimulation of the iPSMCs with vancomycin resulted in marked exocytosis of β-hexosaminidase, whereas no or little release of this enzyme was detected from BMMCs (Fig. 4C and Supplementary Fig. S5C). Therefore, iPSMCs would be potential cell sources for drug-allergy-screening system.

We developed a 2-step differentiation protocol of mast cells from iPS cells. In the conventional method, CTMC-like mast cells are produced from bone marrow cells after 45 days of culture. In contrast, the iPSMCs generated on OP9 cells in the present study were produced after 28 days of culture. Thus, homogeneous CTMC-like mast cells can be easily generated from iPS cells by the OP9 coculture method. On the other hand, Swiss 3T3 coculture methods have different advantage from OP9 coculture systems. The iPSMCs that were cocultured with Swiss 3T3 fibroblasts were more mature than the iPSMCs that were generated on OP9 cells. Because each of these methods has its advantages, the protocol should be chosen in accordance with the intended use.

We successfully developed a 2-step differentiation protocol for generating more mature mast cells from mouse iPS cells. The iPSMCs generated in this study exhibit many characteristics distinct from BMMCs. The iPSMCs possessed the characteristics of mature mast cells, including the heparin contents and degranulation, in response to cationic secretagogues and vancomycin. The iPSMCs serve as an excellent model for in vitro studies of CTMCs. Our results could facilitate clarification of the mechanisms that control the development of mast cells.

Acknowledgments

We thank Dr. S. Yamanaka for kindly providing the mouse iPS cell lines 38C2. We would like to thank Misae Nishijima and Mary S. Saldon (National Institute of Biomedical Innovation) for technical assistance. We thank Dr. Keizo Nishikawa (National Institute of Biomedical Innovation) for helpful discussion.

Author Disclosure Statement

The authors have no financial conflict of interest.

References

1. Metcalfe DD, D Baram and YA Mekori. (1997). Mast cells. Physiol Rev 77:1033–1079.
2. Galli SJ, S Nakae and M Tsai. (2005). Mast cells in the development of adaptive immune responses. Nat Immunol 6:135–142.
3. Kitamura Y. (1989). Heterogeneity of mast cells and phenotypic change between subpopulations. Annu Rev Immunol 7:59–76.
4. Stevens RL and KF Austen. (1989). Recent advances in the cellular and molecular biology of mast cells. Immunol Today 10:381–386.
5. Benoist C and D Mathis. (2002). Mast cells in autoimmune disease. Nature 420:875–878.
6. Bryce PJ, ML Miller, I Miyajima, M Tsai, SJ Galli and HC Oettgen. (2004). Immune sensitization in the skin is enhanced by antigen-independent effects of IgE. Immunity 20:381–392.
7. Lu LF, EF Lind, DC Gondek, KA Bennett, MW Gleeson, K Pino-Lagos, ZA Scott, AJ Coyle, JL Reed, et al. (2006). Mast cells are essential intermediaries in regulatory T-cell tolerance. Nature 442:997–1002.
8. Takano H, S Nakazawa, Y Okuno, N Shirata, S Tsuchiya, T Kainoh, S Takamatsu, K Furuta, Y Taketomi, et al. (2008). Establishment of the culture model system that reflects the process of terminal differentiation of connective tissue-type mast cells. FEBS Lett 582:1444–1450.
9. Wang Y, F Yates, O Naveiras, P Ernst and GQ Daley. (2005). Embryonic stem cell-derived hematopoietic stem cells. Proc Natl Acad Sci U S A 102:19081–19086.
10. Karlsson KR, S Cowley, FO Martinez, M Shaw, SL Minger and W James. (2008). Homogeneous monocytes and macrophages from human embryonic stem cells following coculture-free differentiation in M-CSF and IL-3. Exp Hematol 36:1167–1175.
11. Ledran MH, A Krassowska, L Armstrong, I Dimmick, J Renstrom, R Lang, S Yung, M Santibanez-Coref, E Dzierzak, et al. (2008). Efficient hematopoietic differentiation of human embryonic stem cells on stromal cells derived from hematopoietic niches. Cell Stem Cell 3:85–98.
12. Murry CE and G Keller. (2008). Differentiation of embryonic stem cells to clinically relevant populations: lessons from embryonic development. Cell 132:661–680.
13. Nakano T, H Kodama and T Honjo. (1994). Generation of lymphohematopoietic cells from embryonic stem cells in culture. Science 265:1098–1101.
14. Chadwick K, L Wang, L Li, P Menendez, B Murdoch, A Rouleau and M Bhatia. (2003). Cytokines and BMP-4 promote hematopoietic differentiation of human embryonic stem cells. Blood 102:906–915.
15. Schmitt TM, RF de Pooter, MA Gronski, SK Cho, PS Ohashi and JC Zuniga-Pflucker. (2004). Induction of T cell development and establishment of T cell competence from embryonic stem cells differentiated in vitro. Nat Immunol 5: 410–417.
16. Vodyanik MA, JA Bork, JA Thomson and II Slukvin. (2005). Human embryonic stem cell-derived CD34+ cells: efficient

production in the coculture with OP9 stromal cells and analysis of lymphohematopoietic potential. Blood 105:617–626.
17. Tsai M, J Wedemeyer, S Ganiatsas, SY Tam, LI Zon and SJ Galli. (2000). In vivo immunological function of mast cells derived from embryonic stem cells: an approach for the rapid analysis of even embryonic lethal mutations in adult mice in vivo. Proc Natl Acad Sci U S A 97:9186–9190.
18. Sugiyama D, M Tanaka, K Kitajima, J Zheng, H Yen, T Murotani, A Yamatodani and T Nakano. (2008). Differential context-dependent effects of friend of GATA-1 (FOG-1) on mast-cell development and differentiation. Blood 111:1924–1932.
19. Wiles MV and G Keller. (1991). Multiple hematopoietic lineages develop from embryonic stem (ES) cells in culture. Development 111:259–267.
20. Ma F, N Kambe, D Wang, G Shinoda, H Fujino, K Umeda, A Fujisawa, L Ma, H Suemori, et al. (2008). Direct development of functionally mature tryptase/chymase double-positive connective tissue-type mast cells from primate embryonic stem cells. Stem Cells 26:706–714.
21. Kovarova M, AM Latour, KD Chason, SL Tilley and BH Koller. (2010). Human embryonic stem cells: a source of mast cells for the study of allergic and inflammatory diseases. Blood 115:3695–3703.
22. Okita K, T Ichisaka and S Yamanaka. (2007). Generation of germline-competent induced pluripotent stem cells. Nature 448:313–317.
23. Jincho Y, R Araki, Y Hoki, C Tamura, M Nakamura, S Ando, Y Kasama and M Abe. (2010). Generation of genome integration-free induced pluripotent stem cells from fibroblasts of C57BL/6 mice without c-Myc transduction. J Biol Chem 285:26384–26389.
24. Tchougounova E, G Pejler and M Abrink. (2003). The chymase, mouse mast cell protease 4, constitutes the major chymotrypsin-like activity in peritoneum and ear tissue. A role for mouse mast cell protease 4 in thrombin regulation and fibronectin turnover. J Exp Med 198:423–431.
25. Ohtsu H, A Kuramasu, S Tanaka, T Terui, N Hirasawa, M Hara, Y Makabe-Kobayashi, N Yamada, K Yanai, et al. (2002). Plasma extravasation induced by dietary supplemented histamine in histamine-free mice. Eur J Immunol 32:1698–1708.
26. Wiener Z, M Andrasfalvy, E Pallinger, P Kovacs, C Szalai, A Erdei, S Toth, A Nagy and A Falus. (2002). Bone marrow-derived mast cell differentiation is strongly reduced in histidine decarboxylase knockout, histamine-free mice. Int Immunol 14:381–387.
27. Hosono H, J Aoki, Y Nagai, K Bandoh, M Ishida, R Taguchi, H Arai and K Inoue. (2001). Phosphatidylserine-specific phospholipase A1 stimulates histamine release from rat peritoneal mast cells through production of 2-acyl-1-lysophosphatidylserine. J Biol Chem 276:29664–29670.
28. Fukuda K, M Ohbayashi, K Morohoshi, L Zhang, FT Liu and SJ Ono. (2009). Critical role of IgE-dependent mast cell activation in a murine model of allergic conjunctivitis. J Allergy Clin Immunol 124:827–833 e2.
29. Zsebo KM, J Wypych, IK McNiece, HS Lu, KA Smith, SB Karkare, RK Sachdev, VN Yuschenkoff, NC Birkett, *et al.* (1990). Identification, purification, and biological characterization of hematopoietic stem cell factor from buffalo rat liver—conditioned medium. Cell 63:195–201.
30. Yeatman CF, 2nd, SM Jacobs-Helber, P Mirmonsef, SR Gillespie, LA Bouton, HA Collins, ST Sawyer, CP Shelburne and JJ Ryan. (2000). Combined stimulation with the T helper cell type 2 cytokines interleukin (IL)-4 and IL-10 induces mouse mast cell apoptosis. J Exp Med 192:1093–1103.
31. Hamaguchi Y, Y Kanakura, J Fujita, S Takeda, T Nakano, S Tarui, T Honjo and Y Kitamura. (1987). Interleukin 4 as an essential factor for *in vitro* clonal growth of murine connective tissue-type mast cells. J Exp Med 165:268–273.
32. Hu ZQ, K Kobayashi, N Zenda and T Shimamura. (1997). Tumor necrosis factor-alpha- and interleukin-6-triggered mast cell development from mouse spleen cells. Blood 89:526–533.
33. Yuan Q, MF Gurish, DS Friend, KF Austen and JA Boyce. (1998). Generation of a novel stem cell factor-dependent mast cell progenitor. J Immunol 161:5143–5146.
34. Matsuda H, Y Kannan, H Ushio, Y Kiso, T Kanemoto, H Suzuki and Y Kitamura. (1991). Nerve growth factor induces development of connective tissue-type mast cells *in vitro* from murine bone marrow cells. J Exp Med 174:7–14.
35. Chen CC, MA Grimbaldeston, M Tsai, IL Weissman and SJ Galli. (2005). Identification of mast cell progenitors in adult mice. Proc Natl Acad Sci U S A 102:11408–11413.
36. Arinobu Y, H Iwasaki, MF Gurish, S Mizuno, H Shigematsu, H Ozawa, DG Tenen, KF Austen and K Akashi. (2005). Developmental checkpoints of the basophil/mast cell lineages in adult murine hematopoiesis. Proc Natl Acad Sci U S A 102:18105–18110.
37. Horinouchi Y, K Abe, K Kubo and M Oka. (1993). Mechanisms of vancomycin-induced histamine release from rat peritoneal mast cells. Agents Actions 40:28–36.

Address correspondence to:
Dr. Kenji Kawabata
Laboratory of Stem Cell Regulation
National Institute of Biomedical Innovation
Saito-Asagi 7-6-8
Ibaraki, Osaka 567-0085
Japan

E-mail: kawabata@nibio.go.jp

Received for publication June 18, 2012
Accepted after revision October 8, 2012
Prepublished on Liebert Instant Online October 9, 2012

Stem Cell Reports
Resource
OPEN ACCESS

Long-Term Self-Renewal of Human ES/iPS-Derived Hepatoblast-like Cells on Human Laminin 111-Coated Dishes

Kazuo Takayama,[1,2,3] Yasuhito Nagamoto,[1,2] Natsumi Mimura,[2] Katsuhisa Tashiro,[4] Fuminori Sakurai,[1] Masashi Tachibana,[1] Takao Hayakawa,[5] Kenji Kawabata,[4] and Hiroyuki Mizuguchi[1,2,3,6,*]
[1]Laboratory of Biochemistry and Molecular Biology, Graduate School of Pharmaceutical Sciences, Osaka University, Osaka 565-0871, Japan
[2]Laboratory of Hepatocyte Differentiation, National Institute of Biomedical Innovation, Osaka 567-0085, Japan
[3]iPS Cell-Based Research Project on Hepatic Toxicity and Metabolism, Graduate School of Pharmaceutical Sciences, Osaka University, Osaka 565-0871, Japan
[4]Laboratory of Stem Cell Regulation, National Institute of Biomedical Innovation, Osaka 567-0085, Japan
[5]Pharmaceutical Research and Technology Institute, Kinki University, Osaka 577-8502, Japan
[6]The Center for Advanced Medical Engineering and Informatics, Osaka University, Osaka 565-0871, Japan
*Correspondence: mizuguch@phs.osaka-u.ac.jp
http://dx.doi.org/10.1016/j.stemcr.2013.08.006

SUMMARY

The establishment of self-renewing hepatoblast-like cells (HBCs) from human pluripotent stem cells (PSCs) would realize a stable supply of hepatocyte-like cells for medical applications. However, the functional characterization of human PSC-derived HBCs was not enough. To purify and expand human PSC-derived HBCs, human PSC-derived HBCs were cultured on dishes coated with various types of human recombinant laminins (LN). Human PSC-derived HBCs attached to human laminin-111 (LN111)-coated dish via integrin alpha 6 and beta 1 and were purified and expanded by culturing on the LN111-coated dish, but not by culturing on dishes coated with other laminin isoforms. By culturing on the LN111-coated dish, human PSC-derived HBCs were maintained for more than 3 months and had the ability to differentiate into both hepatocyte-like cells and cholangiocyte-like cells. These expandable human PSC-derived HBCs would be manageable tools for drug screening, experimental platforms to elucidate mechanisms of hepatoblasts, and cell sources for hepatic regenerative therapy.

INTRODUCTION

Human embryonic stem cells (hESCs) and human induced pluripotent stem cells (hiPSCs) have the ability to self-replicate and to differentiate into all types of body cells including hepatoblasts and hepatocytes. Although cryopreserved primary human hepatocytes are useful in drug screening and liver cell transplantation, they rapidly lose their functions (such as drug metabolism capacity) and hardly proliferate in in vitro culture systems. On the other hand, human hepatic stem cells from fetal and postnatal human liver are able to self-replicate and able to differentiate into hepatocytes (Schmelzer et al., 2007; Zhang et al., 2008). However, the source of human hepatic stem cells is limited, and these cells are not available commercially. Therefore, the human pluripotent stem cell (hPSC)-derived hepatoblast-like cells (HBCs), which have potential to differentiate into the hepatocyte-like cells, would be an attractive cell source to provide abundant hepatocyte-like cells for drug screening and liver cell transplantation.

Because expandable and multipotent hepatoblasts or hepatic stem cells are of value, suitable culture conditions for the maintenance of hepatoblasts or hepatic stem cells obtained from fetal or adult mouse liver were developed (Kamiya et al., 2009; Tanimizu et al., 2004). Soluble factors, such as hepatocyte growth factor (HGF) and epidermal growth factor (EGF), are known to support the proliferation of mouse hepatic stem cells and hepatoblast (Kamiya et al., 2009; Tanimizu et al., 2004). Extracellular matrix (ECM) also affects the maintenance of hepatoblasts or hepatic stem cells. Laminin can maintain the character of mouse hepatoblasts (Dlk1-positive cells) (Tanimizu et al., 2004). However, the methodology for maintaining HBCs differentiated from hPSCs has not been well investigated. Zhao et al. (2009) have reported that hESC-derived hepatoblast-like cells (sorted N-cadherin-positive cells were used) could be maintained on STO feeder cells. Although a culture system using STO feeder cells for the maintenance of hepatoblast-like cells might be useful, there are two problems. The first problem is that N-cadherin is not a specific marker for human hepatoblasts. N-cadherin is also expressed in hESC-derived mesendoderm cells and definitive endoderm (DE) cells (Sumi et al., 2008). The second problem is that residual undifferentiated cells could be maintained on STO feeder cells. Therefore, their culture condition cannot rule out the possibility of the proliferation of residual undifferentiated cells. Because it is known that hPSC-derived cells have the potential to form teratomas in the host, the production of safer hepatocyte-like cells or hepatoblast-like cells has been required. Therefore, we decided to purify hPSC-derived HBCs, which can differentiate into mature hepatocyte-like cells, and then expand these cells.

In this study, we attempt to determine a suitable culture condition for the extensive expansion of HBCs derived